FACTA UNIVERSITATIS (NIŠ)
SERIES: ELECTRONICS AND ENERGETICS VOL. 9, NO.1 (1996), 1–12

EDGE-BASED SINGULAR ELEMENTS FOR FINITE–ELEMENT ANALYSIS OF WAVEGUIDES

Zorica Pantić-Tanner and Svetislav Pantić

Abstract. The FEM exhibits a slow rate of convergence when it is used for analysis of waveguides containing sharp edges where electromagnetic field is singular. The convergence of the method can be improved by introducing singular elements that model analytically predicted singular behavior. A number of authors have developed singular elements that are compatible with either scalar or standard vector FEM. In this paper we propose a new singular element that is compatible with the edge-based finite elements of arbitrary order and can cope with any order of singularity while preserving the sparsity of the FEM equations. All necessary integrations are performed in closed form. Edge-based singular elements not only more correctly model singular behavior of the field and thus require smaller FEM mesh, but they also do not introduce any spurious modes in the numerical solution. Numerical results presented in this paper verify that the convergence of the FEM is significantly improved.

1. Introduction

The finite element method (FEM) based on edge elements is a powerful numerical technique for solving a variety of waveguide problems. It is not only capable of handling waveguides of complicated cross-sections and with arbitrary fillings of inhomogeneous media, be they isotropic or anisotropic, but it also eliminates nonphysical, spurious modes from the numerical solution. However, many waveguiding structures contain conducting or dielectric edges embedded in an inhomogeneous isotropic or anisotropic medium, and

---

Manuscript received April 21, 1995.
A version of this paper was presented at the second Conference Telecommunications in Modern Satellite and Cables Services, TELSIKS'95, October 1995, Niš, Yugoslavia..
Dr Z. Pantić–Taner is with School of Engineering San Francisco State University San Francisco, CA 94132, USA. M.S. S. Pantić is with Republic Public Tax Department Center Niš, Strahinjića Bana b.b., Yugoslavia.

the field behavior can be singular in the vicinity of these edges [1], [2]. If polynomial edge-elements are used to model these rapidly varying fields, it becomes necessary to use a fine mesh in the vicinity of the edge [3], [4]. The increase in the number of unknowns in the mesh has the effect of increasing the computational time as well as memory requirements [5]. One way of coping with the singular field behavior is to use covariant-projection elements [6] or edge-based elements [7] that allow the normal component of the field to be discontinuous at a sharp edge. Another way is to augment the trial functions with appropriate singular functions associated with a noodles (unknown) variable [8], [9] which leads to the increase of the bandwidth of the global FEM matrix. The most efficient approach is the use of singular elements. In this case the ordinary elements touching the edge are replaced by singular elements with trial functions that properly model singular field behavior. Singular elements have been used both in scalar [10], [11] and vector [11], [12] FEM formulation.

In this paper a new edge-based element similar to [13] is proposed. This singular element is used in the H-filed FEM formulation [14] and it is compatible with edge elements (specifically the quadratic-normal/liner-tangential edge element). Trial functions are expressed in a triangular polar coordinate system [15] and all the necessary integrations are performed in closed form while the sparsity of the FEM equations is preserved. The number of unknown parameters needed to model the fields is significantly reduced by employing singular elements, as the presented numerical data show, and at the same time the non-spurious modes are eliminated.

2. Finite element formulation

Consider a waveguiding structure uniform along the z-axis of an (x, y, z)-coordinate system. The cross section of the structure (in the xOy plane) is arbitrarily shaped and the material in it is inhomogeneous with $\varepsilon = er(x,y)\varepsilon_0$ and $\mu = \mu_r(x,y)\mu_0$ being permittivity and permeability of the material, respectively; ε_0 and μ_0 are the free space parameters. For a time harmonic excitation of angular frequency ω and the lossless material, the electric, E, and magnetic, H, fields propagating along the z-axis, can be expressed in the following form

$$\begin{aligned} \vec{E} &= E(x,y)e^{j\omega t_e - j\beta_z}, \\ \vec{H} &= H(x,y)e^{j\omega t_e - j\beta_z} \end{aligned} \tag{1}$$

where $\vec{E}, \vec{H}$, are the values of the fields in the cross section $z = 0$ and $\gamma = j\beta$ is the propagation constant.

In this paper a finite element formulation based on the vector Helmholtz equation for magnetic field $\vec{H}$ [16] is used to solve for the modes propagating in the waveguide:

$$\nabla \times \left(\frac{1}{\varepsilon_r} \nabla \times \vec{H} \right) = k_0^2 \mu_r \vec{H} \tag{2}$$

where $k_0^2 = \omega^2 \varepsilon_0 \mu_0$ is the free-space wavenumber. After decomposing the field into a transversal, $\vec{H}_t$, and longitudinal, H_z, components, equation (2) can be separated into two parts, a vector equation that is entirely transverse to a_z, where a_z is the base vector along the z- axis, and a scalar equation that has only z-component

$$\begin{aligned} \nabla_t \times \left(\frac{1}{\varepsilon_r} \nabla_t \times \vec{H}_t \right) - \frac{1}{\varepsilon_r} (j\beta \nabla_t H_z - \beta^2 \vec{H}_t) &= k_0^2 \mu_r \vec{H}_t \\ -\nabla_t \left\{ \frac{1}{\varepsilon_r} (\nabla_t H_z + j\beta \vec{H}_t) \right\} &= k_0^2 \mu_r H_z \end{aligned} \tag{3}$$

where $\nabla_t = a_x \partial/\partial x + a_y \partial/\partial y$ is the transverse delta operator. For convenience, the same scaling as in [5] is introduced:

$$\begin{aligned} \vec{h}_t &= \beta \vec{H}_t, \\ h_z &= -jH_z \end{aligned} \tag{4}$$

and (3) can be rewritten as:

$$\nabla_t \times \left(\frac{1}{\varepsilon_r} \nabla_t \times \vec{h}_t \right) - k_0^2 \mu_r \vec{h}_t = \beta^2 \left(\frac{-1}{\varepsilon_r} \right) (\nabla_t h_z + \vec{h}_t) \tag{5a}$$

$$\nabla_t \left\{ \frac{1}{\varepsilon_r} (\nabla_t h_z + \vec{h}_t) \right\} + k_0^2 \mu_r h_z = 0 \tag{5b}$$

These equations are solved by using FEM with edge-based triangular elements. Within each element field components are expanded in terms of edge-based unknowns and appropriate edge-based shape functions [14]

$$\begin{aligned} \vec{h}_t &= \sum_{i=1}^{K_t} \Psi_i \vec{B}_{ti}(x, y), \\ h_z &= \sum_{i=1}^{K_z} \Lambda_i B_{zi}(x, y) \end{aligned} \tag{6}$$

where $\vec{B}_{ti}(x,y)$ $(i=1,...,K_t)$ and $B_{zi}(x,y)$ $(i=1,...,K_z)$ are vector and scalar basis functions, respectively. A Galerkin procedure is used by testing equation (5a) with vector test functions $\vec{T}_{tj}(x,y)=\vec{B}_{tj}(x,y)$ and equation (5b) with scalar test functions $T_{zj}(x,y)=B_{zj}(x,y)$. The following set of coupled eigen-value equations is produced

$$\begin{bmatrix} C^{tt} & 0 \\ C^{zt} & C^{zz} \end{bmatrix} \begin{bmatrix} \Psi \\ \Lambda \end{bmatrix} = \beta^2 \begin{bmatrix} D^{tt} & D^{tz} \\ 0 & 0 \end{bmatrix} \begin{bmatrix} \Psi \\ \Lambda \end{bmatrix} \tag{7}$$

where

$$\begin{aligned}
C_{ij}^{tt} &= \frac{1}{\varepsilon_r} \iint\limits_{\Delta_l} \left\{ (\nabla_t \times \vec{B}_{ti})(\nabla_t \times \vec{B}_{tj} \right\} ds - k_0^2 \mu_r \iint\limits_{\Delta_e} \left\{ \vec{B}_{ti} \vec{B}_{tj} \right\} dS \\
C_{ij}^{zt} &= \frac{1}{\varepsilon_r} \iint\limits_{\Delta_e} \nabla_t B_{zi} \vec{B}_{tj} dS, \\
C_{ij}^{zz} &= \frac{1}{\varepsilon_r} \iint\limits_{\Delta_e} \nabla_t B_{zi} \nabla_t B_{zj} dS - k_0^2 \mu_r \int\int\limits_{\Delta_e} B_{zi} B_{zj} dS \\
D_{ij}^{tt} &= \frac{-1}{\varepsilon_r} \iint\limits_{\Delta_e} \left\{ \vec{B}_{ti} \vec{B}_{tj} \right\} dS, \\
D_{ij}^{tz} &= \frac{-1}{\varepsilon_r} \iint\limits_{\Delta_e} \vec{B}_{ti} \nabla_t B_{zj} dS
\end{aligned} \tag{8}$$

and Δ_e is the area of the element. This eigenvalue problem is solved iteratively [16], taking advantage of the sparsity of the matrices [C] and [D] [17].

3. Edge-based singular element

Our goal is to construct a singular element which can accurately model singular behavior near a sharp edge (Fig. 1) and at the same time be compatible with an ordinary edge-based element, i.e., produce continuous tangential and allow for discontinuous normal components along the element edges. According to [1], [2] the field in the vicinity of the edge may be singular and in that case behaves as

$$\begin{aligned}
H_z &= d_0 + r^{\tau} a_0(\varphi, z) + r^{\tau+1} a_1(\varphi, z) + r^{\tau+2} a_2(\varphi, z) + \ldots \\
\vec{H}_t &= r^{\tau-1} \vec{b}_0(\varphi, z) + r^{\tau} \vec{b}_1(\varphi, z) + r^{\tau+1} \vec{b}_2(\varphi, z) + \ldots
\end{aligned} \tag{9}$$

where (r, φ, z) is the local polar coordinate system with the origin at the edge as shown in Fig. 1. and the singularity coefficient t depends on the geometry and material properties as described in [18]. Actually, only the transverse component is singular whereas longitudinal component has singular derivative. Moreover, only normal component of the transverse field is allowed to become infinite at the edge while the tangential component stays finite. Singular elements located around the edge are used to model this singular behavior and thus enhance the efficiency of the FEM.

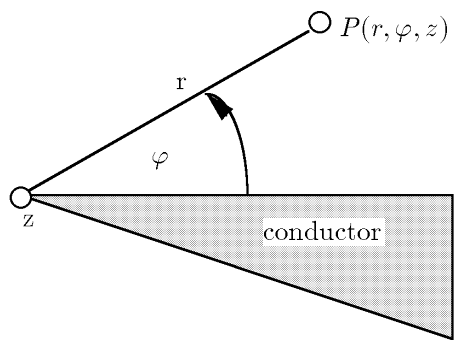

Fig. 1. Conducting edge embedded in dielectric.

A singular element with local numbering of vertices denoted by 1, 2, and 3, with node 1 being the singular point on the edge, is shown in Fig. 2. For convenience we introduce a triangular polar coordinate system (r,s) that is related to the (x,y) coordinates by [15]

$$\begin{aligned} x &= x_1 + \rho\,[x_2 - x_1 + \sigma(x_3 - x_2)] \\ y &= y_1 + \rho\,[y_2 - y_1 + \sigma(y_3 - y_2)] \end{aligned} \tag{10}$$

Hence, the normalized hz field component can be expressed as

$$h_z = f_0 + \rho^{\tau} f_0(\sigma) + \rho^{\tau+1} f_1(\sigma) + \rho^{\tau+2} f_2(\sigma) + \dots \tag{11}$$

In order to model this behavior the approximate h_z is expanded in terms of nodal based unknowns, Λ_i, and singular scalar base (shape) functions, B_i.

$$\begin{aligned} h_z &= \sum_{i=1}^{K} \Lambda_i B_i^M(\rho, \sigma) \\ &= \sum_{m=0}^{M} \sum_{n=0}^{m} \Lambda_{mn} R_m^M(\rho) L_n^m(\sigma) \end{aligned} \tag{12}$$

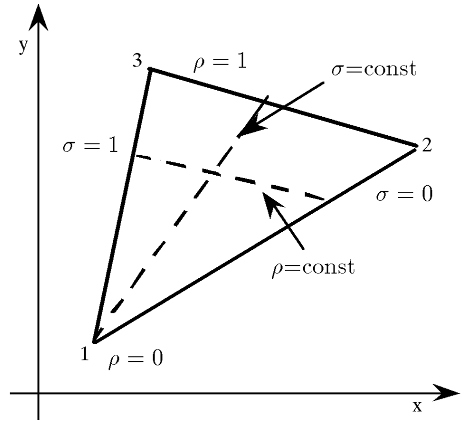

Fig. 2. Singular element with coordinate system.

where coefficient M represents the order of singularity approximation in the radial direction. Distribution of nodes and the relationship between the single (i) and double indexing (m, n) is shown in Fig. 3 for a second order singular element.

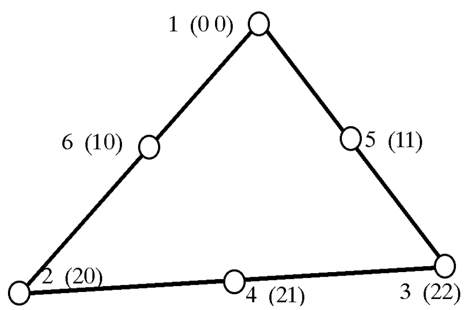

Fig. 3. Single and double node numbering for h_z-base functions in a second order element.

Angular shape functions are usual Lagrange polynomials. Radial shape functions, $R_m^M(\rho)$, represent the singular behavior in the radial direction and have the following form

$$
\begin{aligned}
R_0^M(\rho) &= (1-\rho^\lambda)\prod_{\substack{i=1\\ i\neq m}}^{M} \frac{\rho - \dfrac{i}{M}}{-\dfrac{i}{M}} \\
R_m^M(\rho) &= \frac{\rho^\lambda}{\left(\dfrac{i}{M}\right)^\lambda} L_m^M(\rho)
\end{aligned}
\qquad (13)
$$

such that $R_m^M(\rho)$ is zero at all nodes except at node m and equal to one at the node m.

According to Van Bladel [19] transverse field component in the vicinity of the edge is quasistatic. Hence, we decompose the transverse field in the singular element into a static (singular) and a dynamic (nonsingular) part. In cases when the geometry of the waveguide cross-section supports singular fields they are accurately modeled by the singular (static) part. If the field is non-singular then dynamic part will prevail and again properly model the field behavior. Hence, the transverse field is expressed in terms of edge-based unknowns, Ψ_i, and edge-based vector base functions, $\vec{B}_i$

$$\vec{h}_t = \sum_{i=1}^{N} \Psi_i \vec{B}_i(\rho, \sigma) \tag{14}$$

where a few of the base functions are singular (quasi- static) and the rest of them nonsingular (dynamic). Dynamic functions are the same as standard trial functions for edge-element or have the same behavior along the element edges. Singular functions are quasi-static in nature and can be obtained as a gradient of a linear combination of nodal based scalar functions B_i

$$\begin{aligned} \vec{B}_k &= \nabla_t \sum_{j=1}^{L} c_i B_i^{M_i}(\rho, \sigma) \\ &= \sum_{j=1} c_i \nabla_t B_i^{M_i}(\rho, \sigma) \end{aligned} \tag{15a}$$

and

$$\begin{aligned} B_{mn}^M &= \nabla_t B_{mn}^M \\ &= \frac{l_{23}\vec{n}_{23}}{2\Delta_e} \frac{\partial R_m^M(\rho)}{\partial \sigma} L_n^m(\sigma) - \frac{l_{12}\vec{n}_{12}(1-\sigma)}{2\Delta_e \rho} R_m^M(\rho) \frac{\partial L_n^m(\sigma)}{\partial \sigma} \\ &+ \frac{l_{31}\vec{n}_{31}\sigma}{2\Delta_e \rho} R_m^M(\rho) \frac{\partial L_n^m(\sigma)}{\partial \sigma} \end{aligned} \tag{15b}$$

where $\vec{n}_{12}$, $\vec{n}_{23}$, and $\vec{n}_{31}$ are outward normals with respect to the triangle edges $1-2$, $2-3$, and $3-1$, respectively. Constants c_i in (15a) are chosen in such way that the base function $\vec{B}_k$ has continuous tangential component along the edge it is associated with, and zero tangential components at the other two edges. As explained in [16], using Nedelec conditions [20] a second order standard edge-element was derived with eight vector basis functions: six edge-based and two face-based as shown in Fig. 4. These functions produce quadratic- normal and linear-tangential field along the element edges (QN/LT).

In this case we choose two of the edge-based functions that are associated with the singular node 1, B_3 and B_5, to be singular and the other six nonsingular. These eight functions can be expressed in the triangular polar coordinate system in the following way

$$
\begin{aligned}
\vec{B}_1 &= -\frac{l_{23}}{2\Delta_e} l_{12}\vec{n}_{12}\rho(1-\sigma), \\
\vec{B}_2 &= -\frac{l_{23}}{2\Delta_e} l_{31}\vec{n}_{31}\rho\sigma, \\
\vec{B}_3 &= \nabla_t B_{11}^2 + c\left(\nabla_t B_{11}^1 + \frac{l_{12}\vec{n}_{12}}{2\Delta_e}\right), \\
\vec{B}_4 &= -\frac{l_{31}}{2\Delta_e}\left[l_{23}\vec{n}_{23}\rho\sigma + \frac{l_{12}\vec{n}_{12}(1-\rho)}{2}\right], \\
\vec{B}_5 &= \nabla_t B_{10}^2 + c\left(\nabla_t B_{10}^1 + \frac{l_{31}\vec{n}_{31}}{2\Delta_e}\right), \\
\vec{B}_6 &= -\frac{l_{12}}{2\Delta_e}\left[l_{23}\vec{n}_{23}\rho(1-\sigma) + \frac{l_{31}\vec{n}_{31}(1-\rho)}{2}\right] \\
\vec{B}_7 &= \frac{l_{23}\vec{n}_{23}}{2\Delta_e}\rho 4\sigma(1-\sigma) - \frac{l_{12}\vec{n}_{12}}{2\Delta_e} 4\rho(1-\rho)(1-\sigma) \\
\vec{B}_8 &= \frac{l_{23}\vec{n}_{23}}{2\Delta_e}\rho 4\sigma(1-\sigma) - \frac{l_{31}\vec{n}_{31}}{2\Delta_e} 4\rho(1-\rho)\sigma
\end{aligned}
\tag{16}
$$

where is $c = 2^{\tau+1}/(\tau-1)$. All these base functions produce continuous tangential component and discontinuous normal component along the triangle sides. After substituting these base functions into (8) and performing all the integrations in closed form, element matrices for the singular element were calculated for the appropriate τ.

4. Numerical results

A number typical waveguiding structures containing sharp edges have been analyzed using two approaches. First, only ordinary QN/LT edge-elements have been used, and second, both QN/LT and singular elements have been included. Enhanced convergence of the method using edge-based singular elements have been observed. Numerical results for the propagation constant of different modes in an L-shaped waveguide (Fig. 5) are shown in Table 1. First row for each mode represents values obtained using ordinary

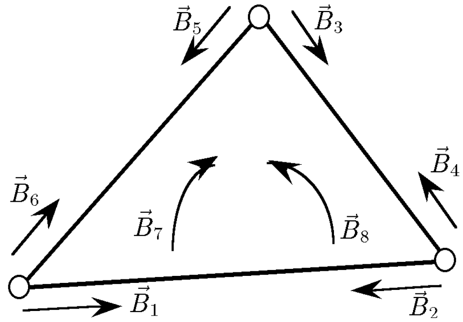

Fig. 4. Definition of vector base functions in a second order QN/LT edge element.

and singular edge-based elements and the second row shows results obtained by using ordinary elements only.

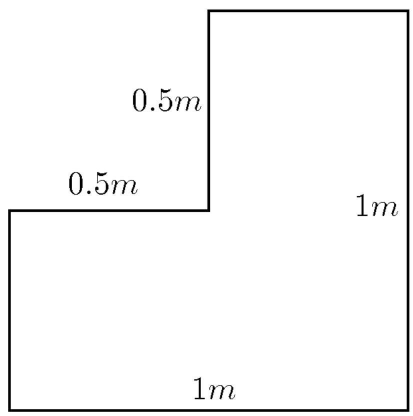

Fig. 5. L–shaped waveguide

It can be noted that the convergence of the results versus the number of used elements is significantly improved by employing singular elements in the vicinity of the metal edge.

5. Conclusions

A new singular element compatible with edge-elements has been derived. It provides continuous tangential and discontinuous normal component along the element edges. Derivation is presented for the singular element that is

Table 1. Propagation constant for first few modes propagating in an L-guide

Mode # and type	Number of Nodes in Mesh 6	20	44	66
1 TE	1.24370	1.21672	1.21537	1.21591
	1.27111	1.22361	1.21871	1.21823
2 TE	1.89215	1.88185	1.88020	1.88010
	1.96794	1.90437	1.88057	1.88041
3 TM	3.31816	3.08623	3.09511	3.09618
	3.37880	3.16381	3.12055	3.09823
4 TE	3.42282	3.15327	3.14324	3.14220
	3.46900	3.17342	3.15444	3.14207
5 TE	3.59736	3.15717	3.14343	3.14226
	3.64270	3.40368	3.15490	3.14346

compatible with QN/LT edge-element. In fact, the field along the edge common with the ordinary element has quadratic normal and linear tangential component whereas it has singular normal and nonsingular tangential component at the edge. Out of eight base functions, six edge-based and two face-based, two are chosen to be singular and in accordance with Van Bladel's paper [19] are quasi-static with zero curl. The other six functions are non-singular, with non-zero curl, and satisfy the same boundary conditions on the edges as ordinary edge-based trial functions. This choice of base functions preserves the sparsity of the FEM equations. All the functions are express in a triangular polar coordinate system which allows one to perform all the necessary integrations in closed form.

A number of typical waveguiding structures has been analyzed and the improved convergence with use of singular elements has been observed. The number of elements needed in the mesh is much smaller if the singular elements are used to model field in the immediate vicinity of the edge. Some numerical results are presented for an L-shaped n.

REFERENCES

1. J. Meixner: *The behaviour of electromagnetic fields at edges.* IEEE Trans. Antennas Propagat., vol. AP-20, pp. 442-446, July 1972.
2. J. Van Bladel: *Singular Electromagnetic Fields and Sources.* Oxford Engineering Science Series 28, Clarendon Press, Oxford, 1991.
3. P. Daly: *Singularities in transmission lines.* in J. R. Whiteman Ed., The Mathematics of Finite Elements and Applications. London:Academic Press, 1973, pp. 337-350.

4. Z. J. Cendes, D. N. Shenton, and H. Shahnasser: *Magnetic field computation using Delaney triangulation and complementary finite element methods.* IEEE Trans. Magn., vol. MAG-19, pp. 2251- 2554, Nov. 1983.

5. J. F. Lee, D. K. Sun, and Z. J. Cendes: *Full-wave analysis of dielectric waveguides using tangential vector finite elements.* IEEE Trans. Microwave Theory Tech., vol. 39, pp. 1262 - 1271, Aug. 1991.

6. R. Miniowitz and J. P. Webb: *Covariant–projection quadrilateral elements for the analysis of waveguides with sharp edges.* IEEE Trans. Microwave Theory Tech., vol. 39, pp. 501-505, Mar. 1991.

7. K. Ise, K. Inoue, and M. Koshiba: *Three–dimensional finite–element method with edge elements for electromagnetic waveguides discontinuities.* IEEE Trans. Microwave Theory Tech., vol. 39, pp. 1289 - 1295, Aug. 1991.

8. J. R. Whiteman: *Finite elements, singularities and fracture.* in J. R. Whiteman Ed., The Mathematics of Finite Elements and Applications III, MAFELAP 1978. London:Academic Press, 1979, pp. 35-54.

9. J. P. Webb: *Finite element analysis of dispersion in waveguides with sharp metal edges.* IEEE Trans. Microwave Theory Tech., vol. 36, pp. 1819 - 1824, Dec. 1988.

10. Z. Pantic and R. Mittra: *Quasi–TEM analysis of microwave transmission lines by the finite–element method.* IEEE Trans. Microwave Theory Tech., vol. 34, 1096-1103, Nov. 1986.

11. J. M. Gill and J. Zapata: *Efficient singular element for finite element analysis of Quasi-TEM transmission lines and Waveguides with sharp metal edges.* IEEE Trans. Microwave Theory Tech., vol. 42, 92 - 98, Jan. 1994.

12. Z. Pantic-Tanner, C. H. Chan, and R. Mittra: *The treatment of edge singularities in the full-wave finite element solution of waveguiding problems.* URSI Symp. Dig., pp. 336, Syracuse, June 1988.

13. Z. Pantic-Tanner, D. R. Tanner, S. A. Savage and A. F. Peterson: *The treatment of edge singularities in waveguiding problems using a finite element method based on edge elements.* URSI Symp. Dig., pp. 90, Newport Beach, June 1995.

14. A. F. Peterson: *Vector finite element formulation for scattering from two-dimensional heterogeneous bodies.* IEEE Trans. Antenna Propagat., vol. 43, pp. 357 - 365, March, 1994.

15. Morris Stern and Eric B. Becker: *A conforming crack tip element with quadratic variation in the singular fields.* Inter. Jour. for Num. Methods in Engi., vol.12, pp. 279 - 288, 1978.

16. Bruce R. Crain, and Andrew F. Peterson: *Analysis of propagation on open microstrip lines using mixed-order covariant projection vector finite elements.* Int. J. of Microwave and Millimeter-Wave Computer-Aided Engin., vol. 5, pp 59 - 67, 1995.

17. O. Osterby and Z. Zlatev: *Direct Methods for Sparse Matrices.* Berlin: Springer-Verlag, 1983.

18. C. H. Chan, Z. Pantic-Tanner and R. Mittra: *Field behaviour near a conducting edge embedded in an inhomogeneous anisotropic medium.* Elect. Lett., vol. 24, pp. 355 - 356, 1988.

19. J. Van Bladel: *Field singularities at metal-dielectric wedges.* IEEE Trans. Antennas Propagat., vol. 33, pp. 450 - 455, 1985.

20. J. C. Nedelec: *Mixed finite elements in R3.* Num. Math., vol. 35, pp. 315 - 341, 1980.